J Solid State Electrochem (2012) 16:1211–1217
DOI 10.1007/s10008-011-1512-7

ORIGINAL PAPER

Electrochemical performance of $LiVPO_4F$/C composite cathode prepared through amorphous vanadium phosphorus oxide intermediate

Xiaochang Qiao · Jiandong Yang · Yaobin Wang · Quanqi Chen · Tingting Zhang · Li Liu · Xianyou Wang

Received: 7 June 2011 / Revised: 18 July 2011 / Accepted: 23 July 2011 / Published online: 9 August 2011

Abstract $LiVPO_4F$/C composites with better electrochemical performance were prepared by calcination of LiF and amorphous vanadium phosphorus oxide (VPO) intermediate synthesized by a sol–gel method using H_3PO_4, V_2O_5 and citric acid as raw materials. The properties of $LiVPO_4F$/C composites were investigated by X-ray diffraction (XRD), scanning electron microscopy (SEM) and electrochemical tests. The analysis of XRD patterns and Fourier transform infrared spectra (FTIR) reveal that VPO intermediate prepared by sol–gel method is amorphous and VPO_4 may exist in VPO intermediate. The compositions of $LiVPO_4F$/C composites are related to the calcination temperature for preparation of amorphous VPO/C intermediate and $LiVPO_4F$/C composite prepared by VPO/C synthesized at 700°C consists of a single crystal phase of $LiVPO_4F$. The electrochemical tests show that $LiVPO_4F$/C composite prepared by VPO/C synthesized at 700°C exhibits higher discharge capacity and excellent cycle performance. This $LiVPO_4F$/C composite displays discharge capacity of 133 mAh g^{-1} at 0.5 C (78 mA g^{-1}) and remains capacity retention of 96.8% after 30 cycles, even at a high rate of 5 C, the composite exhibits high discharge capacity of 115 mAh g^{-1} and capacity retention of 97% after 100 cycles.

X. Qiao · J. Yang · Y. Wang · Q. Chen (✉) · T. Zhang · L. Liu · X. Wang
Key Laboratory of Environmentally Friendly Chemistry and Applications of Ministry of Education, School of Chemistry, Xiangtan University,
Xiangtan, Hunan 411105, China
e-mail: quanqi.chen@yahoo.com

Q. Chen
e-mail: qqchen@xtu.edu.cn

Keywords Electrochemical performance · Lithium vanadium fluorophosphate · Amorphous VPO · Composite cathode

Introduction

Recently, $LiVPO_4F$ [1–10], a polyanion cathode material for lithium-ion batteries first reported by Barker et al. in 2003 [1], has received extensive attention and been considered as an alternative to the presently used $LiCoO_2$ [11, 12] and $LiMn_2O_4$ [13–15]. $LiVPO_4F$ has a triclinic structure, isostructural with the mineral tavorite $LiFePO_4(OH)$ [16] and exhibits a theoretical capacity of about 156 mAh g^{-1}, close to that of the intensively studied $LiFePO_4$ (170 mAh g^{-1}), and a sole discharge voltage plateau of about 4.2 V vs. Li^+/Li, which is higher than that of $LiFePO_4$ (3.5 V) and $LiCoO_2$ (3.9 V). As a result, its theoretical gravimetric energy density is about 10% higher than that of $LiFePO_4$ and $LiCoO_2$. Moreover, as a cathode material, $LiVPO_4F$ exhibits excellent thermal stability as good as that of $LiFePO_4$ [9], and much better than that of its oxide counterparts. But the electric conductivity of $LiVPO_4F$ is much lower than that of oxide cathode materials such as $LiMn_2O_4$ and $LiCoO_2$, and this lower electric conductivity is unfavorable for improvement of its electrochemical performance. Some techniques applied to $LiFePO_4$, such as addition of conductive carbon [17, 18] or/and reduction of particle size, could significantly improve its electric conductivity and result in high electrochemical performance of $LiVPO_4F$.

In previous reports, $LiVPO_4F$/C composites were prepared by two-step [1, 2] or one-step solid-state reaction method [19] and sol–gel method [7]. $LiVPO_4F$/C synthesized by sol–gel method has small particle size and exhibits better electrochemical performance at lower rate (0.2 C),

but it took a longer time to prepare $V_2O_5{\cdot}nH_2O$ gel and dry the mixture of $NH_4H_2PO_4$, $V_2O_5{\cdot}nH_2O$ gel, LiF and carbon, which is not favorable for industrial production. Solid-state reaction methods are convenient for large-scale production of $LiVPO_4F/C$, but the physical mixture of the raw materials could lead to the unevenness in the composition of $LiVPO_4F/C$ composite, which hinders improvement in high rates performance. Zhong et al. [19] used a simple one-step solid-state reaction to synthesize $LiVPO_4F/C$, which has better electrochemical performance than that of $LiVPO_4F/C$ prepared according to the two-step method by calcination of LiF and well-crystallized VPO_4/C, which was produced by sintering the mixture of V_2O_5, $NH_4H_2PO_4$ or $(NH_4)_2HPO_4$ and carbon under inert gas atmosphere at high temperature. The moderate performance at high rates (>1 C) of the $LiVPO_4/C$ synthesized by the above-mentioned methods could be enhanced by modification of synthesis methods. Recently, Makimura et al. [20] found that amorphous VPO_4 prepared by solid-state reaction was much more reactive than the well-crystallized one in the synthesis of cathode material of $Li_5V(PO_4)_2F_2$. In this work, we develop a new route to synthesize $LiVPO_4F/C$ based on a more reactive amorphous vanadium phosphorus oxide (VPO) intermediate prepared using the sol–gel method. Moreover, the electrochemical performance of $LiVPO_4F/C$ was investigated.

Experimental

The amorphous VPO intermediate with 1:1 of molar ratio of V to P was prepared by a sol–gel method.The stoichiometric amount of V_2O_5 and H_3PO_4 was added to citric acid solution, and the mixture solution was strongly stirred for 6 h at 80°C to obtain a greenish black gel. The gel was dried at 80°C in a vacuum oven, ground and pressed into pellets, then sintered for 4 h at 650–750°C in flowing argon to obtain the black VPO/C. The stoichiometric mixture of the prepared VPO/C and LiF was ground, pelletized and then calcined at 750°C for 1 h in flowing argon to obtain the resulting $LiVPO_4F/C$ composite.

During the synthesis of amorphous VPO, citric acid was used as chelating agent as well as reductant for V(V) to lower valent vanadium in sol–gel process, resulting in a homogeneous precursor gel consisting of lower vanadium compounds. Moreover, the dispersive carbon decomposed by citric acid could facilitate the reduction of V(V) or V(IV) compounds, production of VPO and suppression of growth of VPO. The smaller particle size of VPO and dispersive carbon are in favor of the synthesis of smaller $LiVPO_4F/C$ with better electrochemical performance.

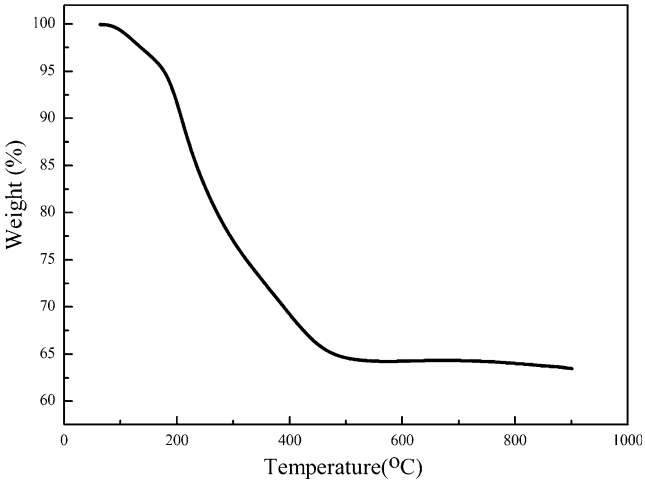

Fig. 1 TG curve for the dried gel

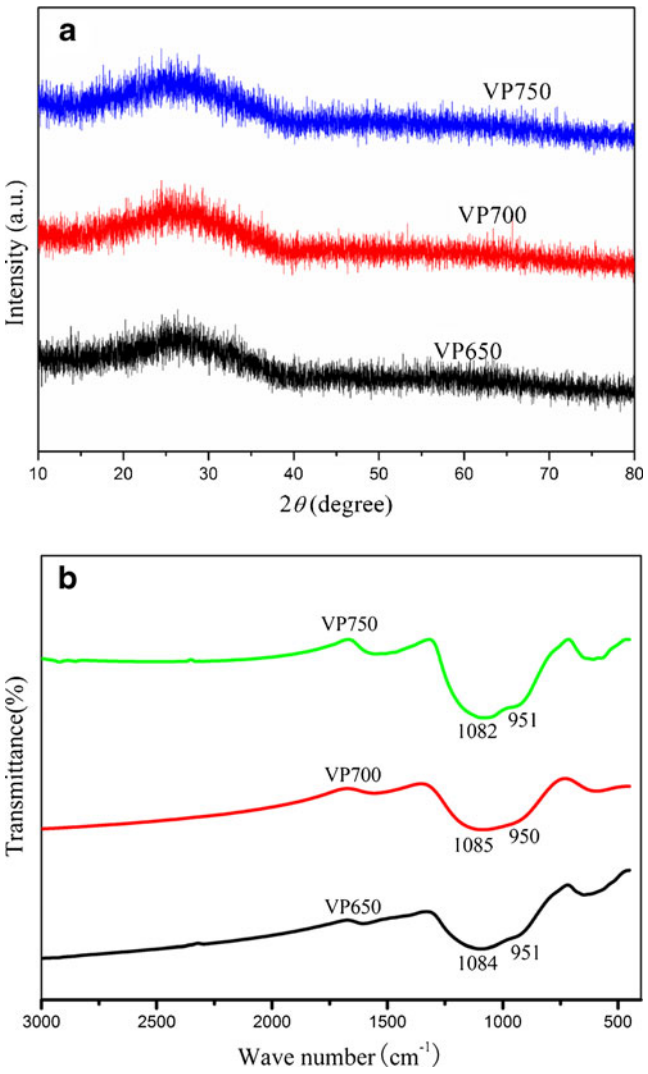

Fig. 2 XRD patterns (**a**) and FTIR spectra (**b**) of the intermediates synthesized at different temperatures

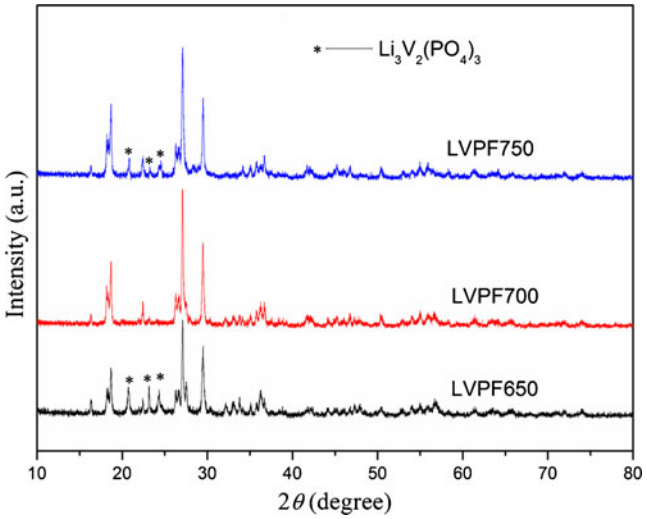

Fig. 3 XRD patterns of composites prepared by calcination of LiF and different amorphous VPO/C intermediates

The crystallinity and structure of samples were characterized by a D/Max III X-ray diffractometer (XRD) with Cu Kα radiation (λ=0.15418 nm). The Fourier transform infrared spectra (FTIR) of the intermediates were recorded with a Bruker IFS113v interferometer. The carbon content of samples was determined by a carbon–sulfur analyzer (Mlti EA2000), and the surface morphology of samples was observed using a SIRION-100 (FEI) scanning electron microscopy (SEM).

The electrochemical tests of $LiVPO_4F$/C samples were carried out using coin cells assembled in an argon-filled glove box. The cathodes consisted of $LiVPO_4F$/C composite materials, polyvinylidiene fluoride (PVDF) binder and acetylene black in a weight ratio of 80:10:10 and were assembled into 2032 size coin cells with lithium as counter electrode, Celgard 2400 separators and a 1 M $LiPF_6$ electrolyte solution in a mixture of ethylene carbonate and dimethyl carbonate (1:1 in volume). In the cycling procedure, the cells were charged with different rates (1 C= 156 mA g^{-1}) to 4.6 V, kept at 4.6 V until 0.02 C rate, and then discharged to 3.0 V at the same rate as charge rate. The electrochemical capacity of samples was calculated based on the mass of the active materials.

Results and discussion

In order to choose the calcination temperature for the dried gel, the thermal decomposition behavior of the dried gel was analyzed by NETZSCHSTA 409 PG/PC thermal analyzer heating from room temperature to 900°C in N_2 atmosphere at a rate of 10°C min^{-1}, and the result is shown in Fig. 1. The TG curve shows that the weight loss of the dried gel occurs at the range of room temperature to 500°C, but when the calcination temperature is higher than 500°C, the weight remains almost constant, suggesting that the formation of stable VPO material may begin at this temperature. Based on the above analysis and the higher calcination temperature in favor of formation of higher conductive carbon, the dried gel was sintered for 4 h at 650, 700 and 750°C, respectively, and the corresponding products were denoted as VP650, VP700 and VP750, respectively.

XRD patterns of VP650, VP700 and VP750 and the corresponding FTIR spectra are shown in Fig. 2. The broad humps in XRD patterns reveal that VP650, VP700 and VP750 are amorphous, similar to the amorphous VPO_4 in a previous report [20]. The FTIR spectra at the bands of about 1,085 and 950 cm^{-1} are consistent with VPO_4 [21], and this amorphous product is made of the elements of V, P, O and C, suggesting that amorphous VPO intermediate comprises PO_4^{3-} and VPO/C intermediate might be a composite of amorphous VPO_4 and carbon. The carbon contents of VP650, VP700 and VP750 are 4.25, 4.02 and 3.95 wt.%, respectively. The final products of $LiVPO_4F$/C composites were prepared by calcination of LiF with stoichiometric amount of VP650, VP700 and VP750 at 750°C for 1 h, respectively, and the corresponding composites were labeled as LVPF650, LVPF700 and LVPF750, respectively. The difference of carbon content between VPO/C intermediate and $LiVPO_4F$/C composites is negligible, justified by the carbon element analysis. The XRD patterns of the final composites shown in Fig. 3 indicate that LVPF650 and LVPF750 composites consist of minor phase of $Li_3V_2(PO_4)_3$ crystal and major phase of $LiVPO_4F$ crystal, isostructural with triclinic $LiFePO_4(OH)$ (PDF 41–1376). Compared with LVPF650 and LVPF750, there is no apparent diffraction peaks of $Li_3V_2(PO_4)_3$ impurity in XRD patterns of LVPF700, suggesting that LVPF700 comprises only $LiVPO_4F$ crystal phase and carbon and this composite may have better electrochemical performance. It is noted that the final products prepared by amorphous VPO intermediates synthesized at 650 and 750°C comprise a certain amount of $Li_3V_2(PO_4)_3$ impurity while $Li_3V_2(PO_4)_3$ is absent in the product synthesized by

Table 1 Cell parameters for composites

Sample	a(nm)	b(nm)	c(nm)	α(°)	β(°)	γ(°)
LVPF650	0.5152(5)	0.5308(3)	0.7465(6)	66.98(2)	67.47(4)	81.74(7)
LVPF700	0.5163(6)	0.5283(2)	0.7489(4)	67.12(5)	66.95(6)	81.63(4)
LVPF750	0.5142(7)	0.5293(5)	0.7451(3)	67.23(4)	67.46(7)	82.00(1)

intermediate prepared at 700°C. The difference of amorphous VPO intermediates may be responsible for this fact. At a calcination temperature of 650°C, the reduction activity of carbon decomposed by organic compounds in dried gel may be not strong enough to completely reduce V (V) or V(IV) to V(III) and produce VPO intermediate with VPO_4 and impurity, resulting in the formation of $Li_3V_2(PO_4)_3$ impurity during the calcination of LiF and VPO intermediate. When the calcination temperature reaches 700°C, the carbon derived from the pyrolysis of organic compounds might be of strong reduction activity to completely reduce higher valent vanadium and form amorphous VPO_4 without impurity. The amorphous VPO_4 is more reactive and in favor of production of a single phase of $LiVPO_4F$ crystal. As calcination temperature approaches 750°C, a small amount of well-crystallized VPO_4 might exist in VPO intermediate, and the somewhat lower reactive well-crystallized VPO_4 might lead to yield impurity of $Li_3V_2(PO_4)_3$ due to the sublimation of VF_3 in the process of incorporation reaction of LiF and VPO_4 [22]. The cell parameters for three composites based on a triclinic structure are listed in Table 1, and the results are similar to the previous report [3].

The SEM images shown in Fig. 4 reveal that particle size of composites decreases with the increasing calcination temperature. The reason for this may be that high calcination temperature favors decomposition of citric acid to smaller residual carbon particles, and the smaller carbon particle as crystal nucleus is beneficial for formation of smaller $LiVPO_4F$/C composite particle. The average particle size of LVPF700 and LVPF750 is 0.5 to 1 μm in diameter. Compared with LVPF650 and LVPF750, LVPF700 has relatively uniform morphology, which might be explained by the fact that LVPF700 composite consists of the lowest content of $Li_3V_2(PO_4)_3$ impurity amongst three composites. Uniform and smaller particle size and lower content of impurity suggest that LVPF700 could exhibit better electrochemical performance.

In order to investigate the electrochemical properties of Li^+ insertion/extraction reactions of LVPF650, LVPF700 and LVPF750 composites, the differential capacity plots were studied based on the initial cycle voltage profiles of composite cathodes in the range of 3.0–4.6 V at a rate of 0.05 C. Figure 5a and b indicates that LVPF650 exhibits charge voltage plateaus of 3.60, 3.70, 4.08, 4.26, 4.29 and 4.50 V during the extraction of lithium ion, and discharge voltage plateaus of 4.17, 4.08, 3.62 and 3.58 V upon the insertion of lithium ion. While the pure $LiVPO_4F$ shows charge voltage plateaus of 4.26 and 4.30 V and discharge voltage plateau of 4.19 V [1], $Li_3V_2(PO_4)_3$ exhibits charge voltage plateaus of 3.60, 3.68, 4.08 and 4.55 V and discharge voltage plateaus of 4.03, 3.65 and 3.57 V, respectively [23].Compared with the electrochemical insertion/extraction properties of $LiVPO_4F$ and $Li_3V_2(PO_4)_3$, Fig. 5a and b reveals that the LVPF650 composite consists of crystal phases of $LiVPO_4F$ and $Li_3V_2(PO_4)_3$, consistent with the results of XRD. Figure 5c and d shows that

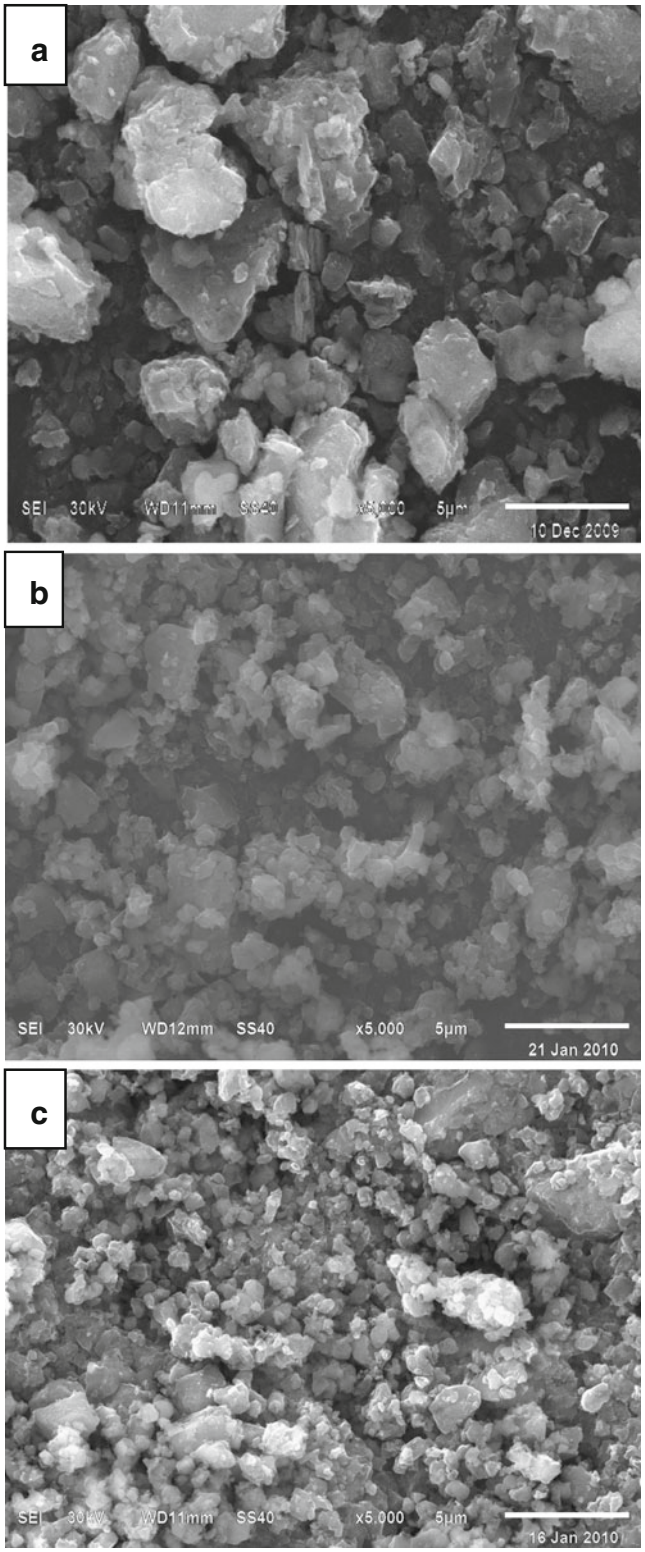

Fig. 4 SEM images of LVPF650 (**a**), LVPF700 (**b**) and LVPF750 (**c**)

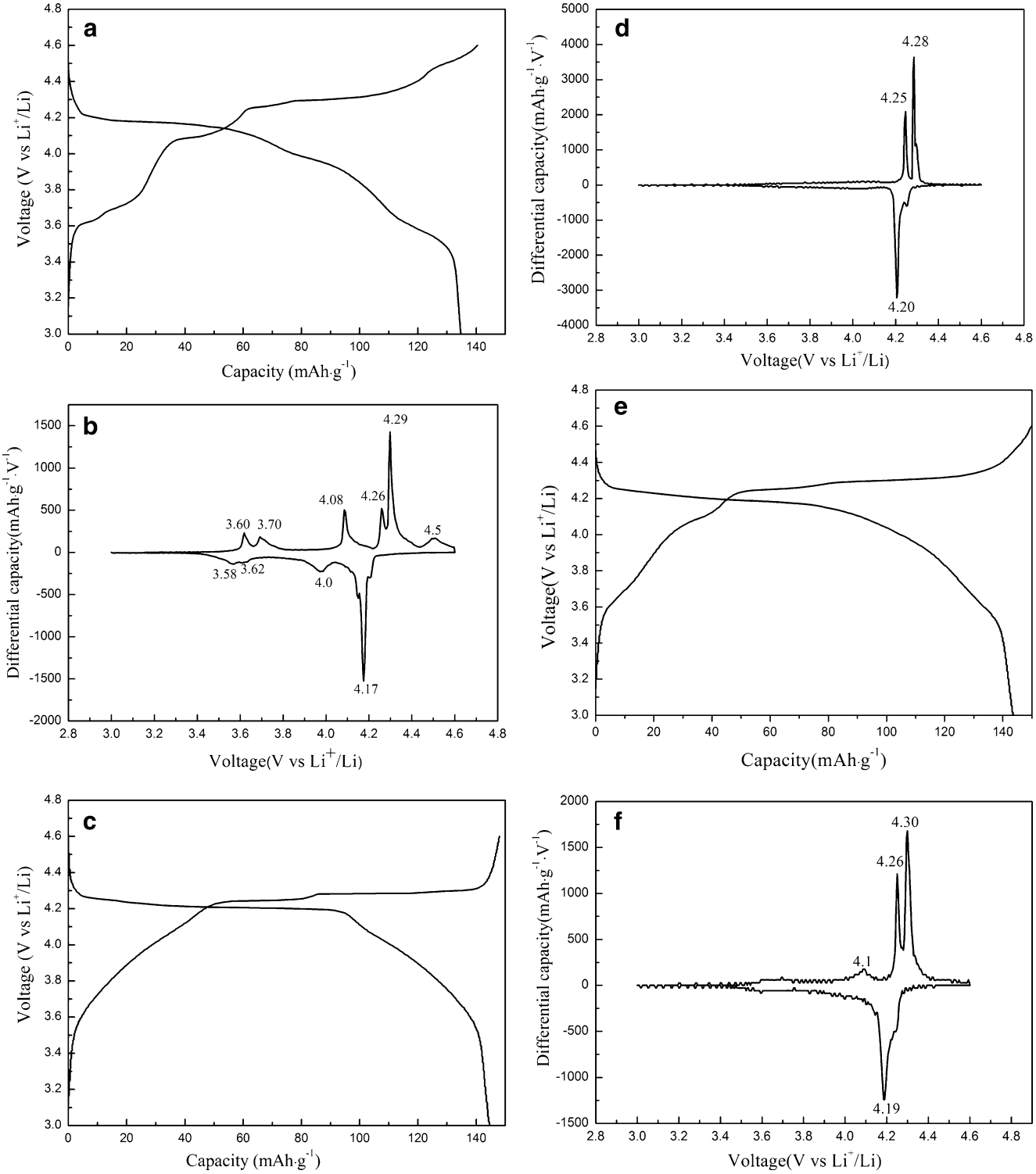

Fig. 5 Initial cycle voltage profiles of LVPF650 (**a**), LVPF700 (**c**) and LVPF750 (**e**) at a rate of 0.05 C; differential capacity plots of LVPF650 (**b**), LVPF700 (**d**) and LVPF750 (**f**)

LVPF700 displays charge voltage plateaus of 4.25 and 4.28 V, and discharge voltage plateaus of 4.20 V, in agreement with the voltage plateaus of $LiVPO_4F$, suggesting that LVPF700 comprises a single crystal phase of $LiVPO_4F$, in agreement with the results of XRD. Figure 5e and f shows that LVPF750 exhibits the charge voltage plateaus of 4.10, 4.26 and 4.30 V and discharge voltage plateau of 4.19 V, indicating that LVPF750 consists of crystal phases of

$LiVPO_4F$ and $Li_3V_2(PO_4)_3$. Voltage profiles shown in Fig. 5a, c and e reveals that the discharge capacities of LVPF650, LVPF700 and LVPF750 are 134.7, 144.5 and 143.2 mAh g^{-1}, respectively, suggesting that LVPF700 and LVPF750 exhibit similar discharge capacity which is much higher than that of LVPF650 at a current rate of 0.05 C.

Initial charge–discharge profiles of LVPF700 and LVPF750 at different rates are shown in Fig. 6a and b, respectively. It can be seen that the discharge capacity decreases with the increasing current rates due to larger polarization in higher current densities. Comparative analysis of Fig. 6a and b reveals that the discharge capacity of LVPF700 is higher than that of LVPF750 at the corresponding current rates. LVPF700 exhibits discharge capacities of 133, 129, 124, 121 and 115 mAh g^{-1} at 0.5, 1, 2, 3 and 5 C, respectively, whereas LVPF750 displays capacities of 128, 124, 115, 111 and 102 mAh g^{-1} at the above-mentioned current rates by sequence, respectively.

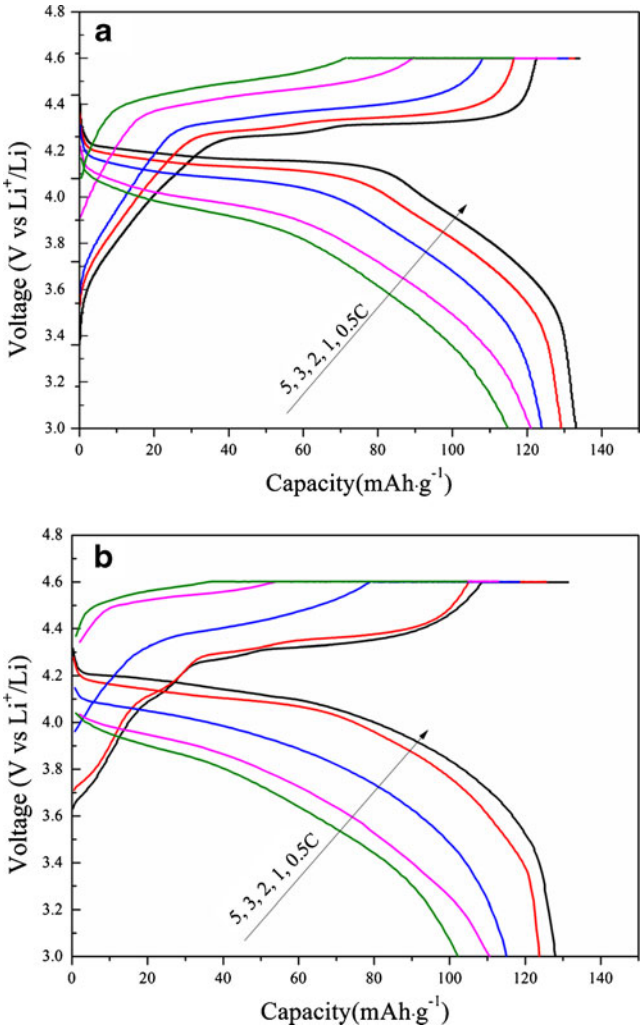

Fig. 6 Initial charge–discharge profiles of LVPF700 (**a**) and LVPF750 (**b**) at different rates

The difference in discharge capacity between LVPF700 and LVPF750 increases with the increasing current rates, indicating that LVPF700 has better rate capability than that of LVPF750.

The cycle performance of LVPF700 and LVPF750 at different rates depicted in Fig. 7 reveals that this two samples exhibit excellent cycle performance. LVPF700 and LVPF750 display initial discharge capacities of 133 and 128 mAh g^{-1} at 0.5 C, respectively, higher than that of $LiVPO_4F$ presented in previous reports [1–8, 10], and the capacity retention rate of 96.8% and 97.0% after 30 cycles, respectively. Even at a high rate of 5 C, LVPF700 presents an initial capacity of 115 mAh g^{-1} and continues to exhibit a capacity of 112 mAh g^{-1} after 100 cycles (capacity retention of 97.4%), while LVPF750 exhibits 99 mAh g^{-1} after 100 cycles and the capacity retention of 97.0%. After over 200 successive cycles from 0.5 to 5 C, LVPF700 and LVPF750 continue to deliver discharge capacities of 130 and 125 mAh g^{-1} when reset to 0.5 C, respectively, indicating that $LiVPO_4F$ has excellent structural stability. The above results and analysis reveal that LVPF700 has a much better electrochemical performance than that of LVPF750.

Conclusions

The $LiVPO_4F$/C composites were prepared by calcination of LiF and amorphous composite of vanadium phosphorus oxide and carbon (VPO/C), which was synthesized by a sol–gel method. The composition of the composites is related to the sintering temperature for synthesis of amorphous VPO/C. The composite prepared via amorphous VPO/C synthesized at 700°C consists of a single crystal phase of $LiVPO_4F$, and this $LiVPO_4F$/C composite

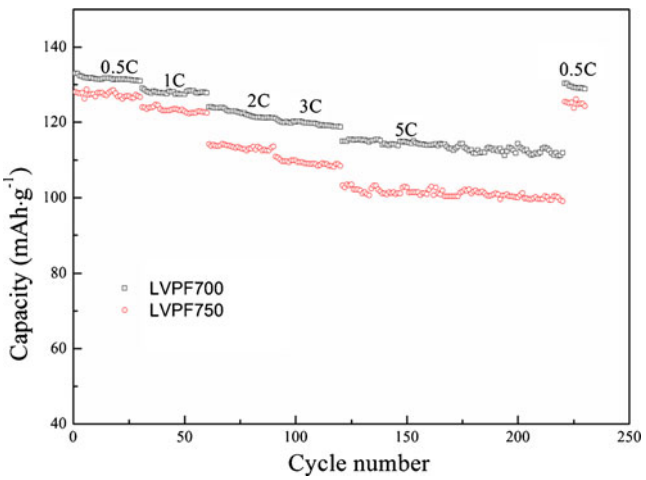

Fig. 7 Cycle performance of LVPF700 and LVPF750 at different rates

exhibits discharge capacity of 133 and 115 mAh g^{-1} at 0.5 and 5 C, respectively, and retains capacity retention of 97.4% at 5 C after 100 cycles. By comparison with the $LiVPO_4F$/C prepared by well-crystallized VPO_4, which is synthesized by solid-state reaction, $LiVPO_4F$/C prepared by amorphous VPO/C exhibits better electrochemical performance, suggesting that it is an effective way to prepare $LiVPO_4F$/C with excellent electrochemical performance using amorphous VPO/C intermediate as raw material.

Acknowledgements The authors gratefully acknowledge financial support from the NSFC (No. 20871101) and the Scientific Research Fund of Hunan Provincial Education Department (No. 09C947).

References

1. Barker J, Saidi MY, Swoyera JL (2003) J Electrochem Soc 150: A1394–A1398
2. Barker J, Saidi MY, Swoyer JL (2004) J Electrochem Soc 151: A1670–A1677
3. Barker J, Gover RKB, Burns P, Bryan A, Saidi MY, Swoyer JL (2005) J Power Sources 146:516–520
4. Gover RKB, Burns P, Bryan A, Saidi MY, Swoyer JL, Barker J (2006) Solid State Ionics 177:2635–2638
5. Barker J, Saidi MY, Gover RKB, Burns P, Bryan A (2007) J Power Sources 174:927–931
6. Reddy MV, Subba Rao GV, Chowdari BVR (2010) J Power Sources 195:5768–5774
7. Li Y, Zhou Z, Gao XP, Yan J (2006) J Power Sources 160:633–637
8. Zhong S, Yin Z, Wang Z, Chen Q (2007) Rare Met 26:445–449
9. Zhou F, Zhao X, Dahn JR (2009) Electrochem Commun 11:589–591
10. Zhang Q, Zhong S, Liu L, Liu J, Jiang J, Wang J, Li Y (2009) J Phys Chem Solids 70:1080–1082
11. Porthault H, Le Cras F, Franger S (2010) J Power Sources 195:6262–6267
12. Park JH, Kim JS, Shim EG, Park KW, Hong YT, Lee YS, Lee SY (2010) Electrochem Commun 12:1099–1102
13. Lewandowski A, Swiderska Mocek A, Swiderska Mocek I (2010) Electrochim Acta 55:1990–1994
14. Karthick SN, Richard Prabhu Gnanakan S, Subramania A, Subramania HJ (2010) J Alloys Compd 489:674–677
15. Yue H, Huang X, Lv D, Yang Y (2009) Electrochim Acta 54:5363–5367
16. Loiseau T, Calage Y, Lacorre P, Férey G (1994) J Solid State Chem 111:390–396
17. Ting-Kuo Fey G, Lu TL, Wu FY, Li WH (2008) J Solid State Electrochem 12:825–833
18. He YB, Ling GW, Tang ZY, Song QS, Yang QH, Chen W, Lv W, Su YJ, Xu Q (2010) J Solid State Electrochem 14:751–756
19. Zhong S, Wang J, Li Y, Liu L, Liu J, Yang J (2009) Chem Lett 38:374–375
20. Makimura Y, Cahill LS, Iriyama Y, Goward GR, Nazar LF (2008) Chem Mater 20:4240–4248
21. Baran EJ, Muto F, Kumada N, Kinomura N (1989) J Mater Sci Lett 8:1305–1306
22. Barker J, Gover RPK, Burns P, Bryan A, Saidi MY, Swoyer JL (2005) J Electrochem Soc 152:A1776–A1779
23. Saidi MY, Barker J, Huang H, Swoyer JL, Adamson G (2003) J Power Sources 119–121:266–272